



## Green Production of Chitin from Black Soldier Fly Pupae Using a Natural Deep Eutectic Solvents

Nila Tanyela Berghuis<sup>1,\*</sup>, Raisya Salsabila<sup>1</sup>, Shanny Fridarima<sup>1</sup>,  
 Ananda Azhari Aprianty Pabo<sup>1</sup>, Intan Puspita Sari<sup>1</sup>



<sup>1</sup> Study Program of Chemistry, Faculty of Science and Computer, Universitas Pertamina, Jakarta 12220, Indonesia

\* Corresponding author: [nila.tanyela@universitaspertamina.ac.id](mailto:nila.tanyela@universitaspertamina.ac.id)

<https://doi.org/10.14710/jksa.26.11.437-444>

### Article Info

#### Article history:

Received: 11<sup>th</sup> September 2023

Revised: 24<sup>th</sup> November 2023

Accepted: 21<sup>st</sup> December 2023

Online: 25<sup>th</sup> December 2023

#### Keywords:

Black Soldier Fly (BSF); Chitin;  
 NADES; Isolation

### Abstract

Natural deep eutectic solvents (NADES) are eco-sustainable, non-toxic, non-volatile, renewable, reusable, and biodegradable, and are composed of natural compounds. NADES were developed as a new-generation solvent for extracting chitin from black soldier fly (BSF) pupae, and its effectiveness for demineralization and deproteinization was determined. Here, two promising NADES, consisting of mixtures of choline chloride–betaine–xylitol (NADES A) and choline chloride–malic acid–water (NADES B), were tested. Fourier transform infrared (FTIR) spectroscopy, thermogravimetric analysis (TGA), X-ray diffraction (XRD), and scanning electron microscopy (SEM) were used to investigate the changes in the chemical composition of the extracted chitin.  $\alpha$ -chitin revealed at wavenumbers 1660–1500  $\text{cm}^{-1}$ , in the amide group and decomposed at 330–350°C. NADES A and NADES B have a crystalline index of 91.65% and 90.65%, respectively. The chitin–NADES A and chitin–NADES B surfaces reveal the repetition of square, pentagonal, and hexagonal units (250 $\times$  magnification) and fibrils (25,000 $\times$  magnification). This study provides a green approach for chitin production from BSF and reveals the potential of NADES for extracting bio-polymers from natural sources.

### 1. Introduction

After cellulose, chitin, known as poly (b-(1-4)-N-acetyl-D-glucosamine, is the second most common chemical. Excellent qualities of biodegradability, bio-compatibility, renewability, and non-toxicity characterize chitin and its derivatives, such as chitosan [1]. It is also insoluble in water and various organic solvents due to its high degree of crystallinity and strong hydrogen bonding between its chains. Hence, chitin and its derivatives find extensive use in various industries, including paper, plastics, bioengineering, food, textiles, medical/bio-materials, adsorbents, and cosmetics [2]. By 2027, the chitin market is predicted to reach USD 2.941 billion [3]. The waste of crustaceans, like shrimp and crab shells, is used to extract chitin that is sold commercially [4]. However, different crab species have different chitin contents and physicochemical characteristics. Also, crustaceans are vulnerable to seasonality and low

reproductive rates, and such changes in raw materials are generally unfavorable for industry [5].

Insects, unlike crustaceans, are not seasonal and reproduce quickly due to their high reproductive rate. Insect molts can contain up to 35% dry weight of chitin, depending on the species [6]. It is well known that flies, particularly the black soldier fly, are biodegradable organic waste species. Native to North America, the black soldier fly (BSF) is an excellent environmentally friendly [7]. BSF is the most popular insect species worldwide [8]. It can generate a significant volume of biological wastes, specifically puparium and dead adults, annually due to BSF's short life cycle. They can pollute the environment if not handled correctly [9]. This process' waste can provide free chitin all year long.

The BSF life is categorized into five stages: egg, larva, prepupa, pupae, and fly. The life cycle of BSF begins from egg hatching and produces larvae that transform into prepupae within 14 days to 2 months, alternating

according to growth conditions [10]. These cyclical transitions produce shedding, the first chitin-rich byproduct. Shedding is the epidermal layer of BSF larvae. Over time, the bright brown prepupae turns dark brown and eventually black [11]. The pre-pupae are the second byproduct that is rich in chitin. Subsequently, the prepupae become pupae by converting soft tissues from larvae to flies. After ten days, the fly crawls out and leaves behind an empty shell called a cocoon [8], which is the third byproduct rich in chitin. The fly lives only a few days to lay eggs and then dies. BSF contains up to 8% and 24%, with shedding and cocoon being the most chitin-rich [12].

Chitin can be isolated in two stages: demineralization and deproteinization. Generally, chitin isolation is done by conventional chemical methods. However, the treatment includes strong acids and alkalis at high temperatures that produce waste with high environmental toxicity. In addition, this process requires large amounts of water for the neutralization stage between the acid and base treatments, high temperatures, and long reaction times [13]. All these factors limit the sustainability of conventional chemical methods. Alternatively, biological methods utilizing enzymatic reactions and microbial fermentation are used. Still, the drawback of this method is the range of time in the fermentation cycle and the high cost of the enzyme [13, 14, 15]. The low efficiency of demineralization and deproteinization and the challenges for large-scale processing are the weaknesses of chitin isolation by biological methods. Therefore, chitin is isolated with ionic liquids, considering their low vapor pressure, non-flammability, and good solubility. However, ionic liquids have been reported to have harmful effects, such as toxicity and non-biodegradability [14].

Natural deep eutectic solvents (NADES) are a promising eco-friendly and sustainable method due to their safe multi-component eutectic mixtures with low melting points [16]. The components of NADES consist of hydrogen bond acceptors (HBAs) and hydrogen bond donors (HBDs) [17]. Generally, the HBAs and HBDs used are derived from natural compounds, especially primary metabolites, including organic acids, sugars, and amino acids, with a molar ratio of 1:2 [18]. However, the molar ratio can be different depending on the solubility. NADES are biocompatible, sustainable, biodegradable, non-volatile, low-cost, and simple to manufacture [19]. These properties make NADES a potential solvent for chitin isolation. Generally, the NADES component used for chitin isolation consists of ChCl/organic acid due to its low toxicity and ability to remove calcium carbonate.

According to research by Huang *et al.* [18], chitin isolation using ChCl/malic acid can remove most minerals and proteins. Using NADES in chitin isolation is a superior method to other methods. Betaine can also be used as a hydrogen bond acceptor (HBA) for chitin isolation with other components such as HBDS, organic acids, and alcohols. Rodrigues *et al.* [20] mentioned that using water in NADES for chitin isolation can increase efficiency. Because the presence of water can facilitate mineral removal and protein hydrolysis, based on this background, this study divided NADES into two types:

NADES A (xylitol–betaine–choline chloride) and NADES B (choline chloride–xylitol–water) with a certain ratio based on their solubility to extract chitin from BSF pupae. More specifically, to evaluate their properties, chitin samples purified from BSF biomass with NADES A and NADES B were tested using FTIR, XRD, TGA, and SEM.

## 2. Experimental

### 2.1. Materials and Instrumentation

Chemicals such as choline chloride (Sigma–Aldrich), betaine monohydrate  $\geq 99.9\%$  (Sigma–Aldrich), xylitol  $\geq 98.9\%$  (Sigma–Aldrich), sodium hydroxide (analytical grade, Merck–EMSURE), sodium hydroxide (PT. Pasifik Kimia Indonesia), ethanol (analytical grade, Merck–Supelco), chitin extra pure (LOBA CHEMIE PVT. LTD.), silica gel (CAT. 297–011–020R), and distilled water were used to produce NADES solvent and to isolate the chitin compound from BSF which collected by Putra Maggot Tangerang. The instruments used were a rotary evaporator (Heidolph, Hei–VAP Value G3 Vertical), hotplate (Thermo Scientific, CIMAREC+), analytical balance (FUJITSU FSR–A220), refractometer (KRÜSS DR201–95), Oven (redLINE by BINDER RL12–16015), and vacuum pump gas (Gilson, DOA–P504 BN).

### 2.2. Synthesis of NADES

This study synthesized NADES by mixing choline chloride, betaine, xylitol, and malic acid with the molar ratio in Table 1. ChCl is a hygroscopic material; it was placed in a glass desiccator with silica gel for 24 hours before use to remove any moisture content. The HBD and the HBA were weighted using an analytical balance with 0.0001 g precision and then placed in a 100 mL Schott bottle and dried in an oven at 90–110°C for 15 minutes to remove any water droplets. Afterward, the specified molar proposition and the mixed solution were heated for 1–2 hours, at 50–90°C, in a water bath with continuous agitation at a constant rotational speed of 250 rpm until the transparent liquid was obtained. The liquid of NADES was stored at room temperature.

**Table 1.** The composition of NADES A and NADES B

Sample	Composition	Ratio
NADES A	Choline chloride: betaine: xylitol	1:1:1
NADES B	Choline chloride: malic acid: water	1:1:2

### 2.3. Extraction of Chitin from Black Soldier Fly

The pretreated BSF powder was weighed and dispersed with various NADES solvents. Then, the mixture was heated on a hotplate for at least 2 hours with continuous agitation at a constant rotating speed of 200 rpm. The chitin was filtered using a Buchner funnel containing Whatman paper No. 42 and washed using distilled water until the chitin was neutral. The remaining NADES were collected for further use. After separation, the chitin was dried in an oven at 55°C. The chitin yield was evaluated by calculating the weight ratio of extracted chitin to raw prepupae BSF.

### 2.4. NADESs Viscosity and Density

The intrinsic viscosity of DESs was determined using a Cannon–Fenske viscometer (Gratech, Type No. 513 03) at room temperature (24°C). NADES were inserted into the Cannon–Fenske viscometer and sucked using a bulb to the upper limit. Then, NADES were allowed to flow to the lower limit. The flow rate time was recorded, and the experiment was repeated three times.

The intrinsic density of NADES was determined using a 10 mL Pycnometer (Gratech). An empty pycnometer was weighed with an analytical balance. The pycnometer was filled with NADES and then weighed. The weight difference is calculated, and the density is determined using Equations (1) and (2).

$$\eta_{NADES-n} = \frac{t_{NADES-n} \times \rho_{NADES-n}}{t_{water} \times \rho_{water}} \times \eta_{water \text{ at } 25^\circ\text{C}} \quad (1)$$

$$\rho_{NADES-n} = \frac{m_{NADES-n}}{m_{water}} \times \rho_{water \text{ at } 25^\circ\text{C}} \quad (2)$$

### 2.5. Characterization of Extracted Chitin

#### 2.5.1. Fourier-Transform Infrared Spectroscopy (FTIR)

The purified chitin samples were measured in a Nicolet iS5 spectrometer (Thermo Scientific, USA) equipped with an iD7 ATR accessory. The spectra were recorded in the wavelength range of 4000 cm<sup>-1</sup> and 400 cm<sup>-1</sup>.

#### 2.5.2. Thermogravimetric Analysis (TGA)

TGA curve was obtained using Discovery Thermal Analysis 650 SDT. Pre-weighed chitin samples (about 1000 mg) were analyzed in the temperature ramp from 20 to 800°C at 10°C min<sup>-1</sup> in a nitrogen atmosphere with a flow of 50 mL min<sup>-1</sup>.

#### 2.5.3. X-ray Diffraction (XRD)

XRD measurement was performed at 2θ with a Cu-Kα radiation source, a scanning speed of 10° min<sup>-1</sup>, and a scanning angle from 3–45° using Rigaku of the 6th generation MiniFlex. Chitin crystals are calculated using Equation (3).

$$x_c(\%) = \frac{A_c}{A_c + A_d} \times 100\% \quad (3)$$

#### 2.5.4. Scanning Electron Microscope (SEM)

SEM was employed to analyze the surface structure of BSF chitin after the samples were coated with Pt/Au

using a Scanning Electron Microscope (JEOL JSM–6510 LA) operated at 250× and 25,000× magnifications.

## 3. Results and Discussion

### 3.1. Synthesis of NADES

In this study, the synthesis NADES is made up of mixing two or more components, HBA and HBD, in their solid or liquid form, capable of associating via hydrogen bonds. Both HBD and HBA were combined by proper mixing and heating to form a liquid mixture with a melting point lower than the individual components called eutectic temperature [21]. Visualization of interactions in NADES A and NADES B can be seen in Figure 1.

Density and viscosity are the most important physical properties of NADES. NADES have a higher density than water. The carbon chain length influences the density of NADES and the number of hydroxyl groups contained therein [22]. Among NADES, NADES B has a higher density than NADES A. It can occur due to differences in the degree of hydrogen bonding in NADES. The minor degree of hydrogen bonding indicates that the liquid is highly organized, and the bonds are connected through stronger interactions. Consequently, a much smaller space is formed in its structure, leading to an increased density of NADES [23]. As shown in Table 2, the viscosity of NADES B has a smaller value than that of NADES A due to their different components. In the case of NADES B, the presence of a water component contributes to viscosity reduction [24]. This effect occurs because water tends to weaken the interactions between the components [25].

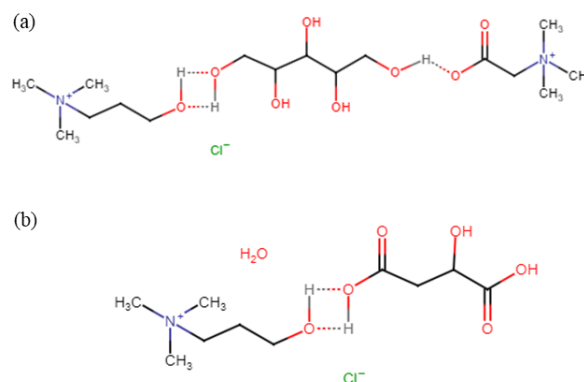


Figure 1. Interaction between components of (a) NADES A, (b) NADES B

Table 2. The properties of NADES A and NADES B

Sample	Density (g/cm <sup>3</sup> )	Viscosity (mPa.s)
NADES A	0.99	3.39
NADES B	1.09	2.43

### 3.2. Fourier-Transform Infrared Spectroscopy

FTIR spectra of NADES (Figure 2) with different component compositions show strong absorption bands at wavenumbers 3307, 3339, and 1638  $\text{cm}^{-1}$ . Wavenumbers 3307 and 3339  $\text{cm}^{-1}$  show the vibrations of the O-H stretching group formed. Wavenumbers 1638 and 1714  $\text{cm}^{-1}$  are C-O stretching absorption bands that indicate the formation of hydrogen bonds between precursors. The absorption band at 1638  $\text{cm}^{-1}$  is associated with angular deformation of the O-H group of water molecules contained in NADES [23, 26, 27]. A summary of bond vibration value data is in Table 3.

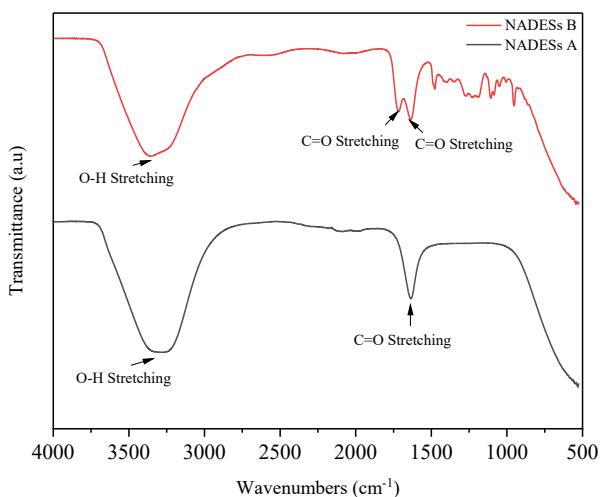


Figure 2. FTIR spectra of NADES A and NADES B

Table 3. Vibration modes of NADES A and NADES B

Vibration mode	Wavenumber ( $\text{cm}^{-1}$ )	
	NADES A	NADES B
O-H stretching	3307	3339
C-O stretching	1638	1638, 1714

Figure 3 shows the ATR-FTIR spectrum of the chitin extracted with NADES, chitin-NADES A, and chitin-NADES B. It shows peaks at wavenumber 3435  $\text{cm}^{-1}$  for O-H stretching vibration and 3256 and 3103  $\text{cm}^{-1}$  for N-H stretching vibrations. These peaks are similar to research by Koshy *et al.* [28]. At the same time, two peaks at wavenumbers 2925 and 2854  $\text{cm}^{-1}$  show C-H vibrations consisting of  $\text{CH}_2$  and  $\text{CH}_3$ . The range of wavenumbers 1660-1500  $\text{cm}^{-1}$  indicates the presence of amide groups, such as amide I and amide II. Wavenumbers 1651 and 1619  $\text{cm}^{-1}$  indicate amide I, revealing  $\alpha$ -chitin [29]. Meanwhile, amide II is detected at wavenumber 1549  $\text{cm}^{-1}$ . Furthermore, two other peaks at wavenumbers 1440 and 1370  $\text{cm}^{-1}$  show the asymmetric deformation of  $\text{CH}_3$ . Meanwhile, the wavenumber 1014  $\text{cm}^{-1}$  shows C-O stretching vibrations. The FTIR spectra of chitin produced in this study are similar to previous studies using different shells [28, 30, 31, 32] and chitin isolated from BSF pupae [29, 33, 34]. A summary of bond vibration value data is in Table 4.

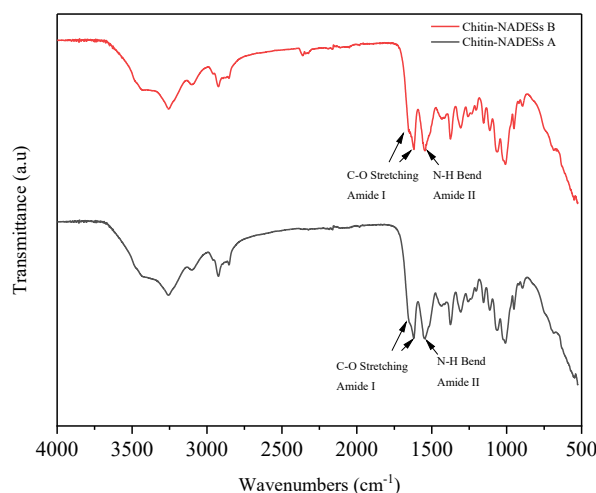


Figure 3. FTIR spectrum of chitin-NADES A and chitin-NADES B

Table 4. Vibration modes of NADES A and NADES B

Vibration mode	Wavenumber ( $\text{cm}^{-1}$ )	
	Chitin-NADES A	Chitin-NADES B
O-H stretching	3456	3456
N-H stretching	3253	3253
	3095	3095
Symmetric $\text{CH}_3$ stretching and asymmetric $\text{CH}_2$ stretching	2925	2925
	2834	2834
C=O stretching (amide I)	1670	1670
	1613	1613
N-H bending (amide II)	1546	1534
	1444	1444
C-H bending	1376	1376
	1025	1003
C-O stretching	1025	1003

### 3.3. Thermogravimetric Analysis

TGA analysis aims to determine the thermal stability of the BSF pupae-based chitin samples. Figure 4 shows the TGA and DTG curves for the chitin samples extracted with NADES A and NADES B, respectively. In these curves, both samples experienced two degradations. The first degradation occurred in the temperature range of 50°C to 100°C, indicating the evaporation of water [35]. The second degradation experienced a significant weight loss, indicating the decomposition of the main chitin chain [30], where the degradation is caused by dehydration of the saccharide ring [36].

Thermal stability was assessed based on the maximum degradation temperature ( $T_m$ ) value. The maximum degradation temperature of chitin-NADES A was 374.55°C. In comparison, the maximum degradation temperature of chitin-NADES B was 363.67°C. Based on these data, chitin-NADES A has a greater maximum degradation temperature value than chitin-NADES B. This shows that chitin extracted from NADES A has a higher maximum degradation temperature. This indicates that chitin extracted with NADES A undergoes less demineralization and deproteination than chitin extracted with NADES B. More minerals and proteins in chitin-NADES A will affect the molecular weight. Thus, degrading the sample requires greater energy [37]. Based on the thermal stability data, it is also concluded that chitin extraction with NADES B is much better than NADES A. This aligns with research conducted by Huang *et al.* [18] that chitin extraction is more effective using ChCl and organic acids. In addition, based on the research of Saini *et al.* [38] the presence of water in the synthesis of NADES leads to a reduction in viscosity, resulting in higher extraction efficiency for NADES B.

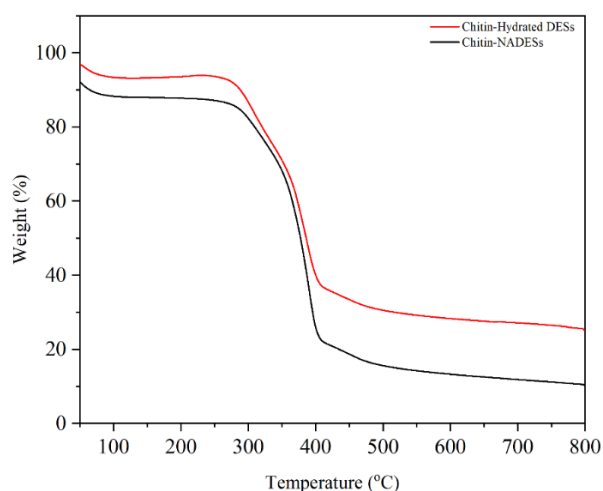


Figure 4. TGA curves of chitin-NADES A and chitin-NADES B

### 3.4. X-ray Diffraction

The crystallinity of chitin was measured under the curve for  $3^\circ \leq 2\theta \leq 45^\circ$ , based on a method proposed for cellulose and used here for chitin [39]. It is configured with a copper source, providing X-rays with a wavelength of 1.54 Å. The  $2\theta$  positions of diffraction peaks are directly proportional to the wavelength of the incoming X-rays ( $\lambda$ ) according to the Bragg equation:  $n\lambda = 2d\sin\theta$  [40]. XRD was used to confirm the  $\alpha$ -,  $\beta$ -, and  $\gamma$ -forms of the chitin extracted from BSF.  $\alpha$ -chitin is characterized by sharp peaks, while broader peaks represent  $\beta$ - and  $\gamma$ -chitin. Previous studies have shown that the peaks of the three forms of chitin are in the range of 9–29° [4, 41, 42, 43, 44].

XRD involves the diffraction of X-rays by a crystal structure in the sample. Figure 5 visualizes the XRD diffractograms of chitin-NADES A and chitin-NADES B. chitin-NADES A showed two sharp peaks at 9.46° and 19.42° and weak peaks at 12.70° and 22.86°, confirming the  $\alpha$ -form of the chitin polymer [4, 45]. The peak also appears on chitin-NADES B. It showed two sharp peaks at 9.40° and 19.46° and weak peaks at 12.84° and 23.34°. Meanwhile, peak 26.56° (chitin-NADES A) and 26.40° (chitin-NADES B) shows the  $\beta$ -form, proven by Jang *et al.* [45] in their research. These chitin peaks were very similar to those of other insect species [46, 47, 48, 49] and *Hermetia illucens* itself [4, 41, 42, 43, 44] in the range of 9–29°.

The degree of crystallinity of chitin-NADES A and chitin-NADES B are 91.65% and 90.65%, respectively. At the same  $2\theta$  range ( $3^\circ \leq 2\theta \leq 45^\circ$ ), the degree of crystallinity has the same value as the study by Soetemans *et al.* [12]. Triunfo *et al.* [44] stated that the degree of crystallinity of insect chitin is in the range of 40 to 90%, mainly 60–80%. The degree of crystallinity can be affected by the source or species, gender, growth stage, and preparation or purification process [44].

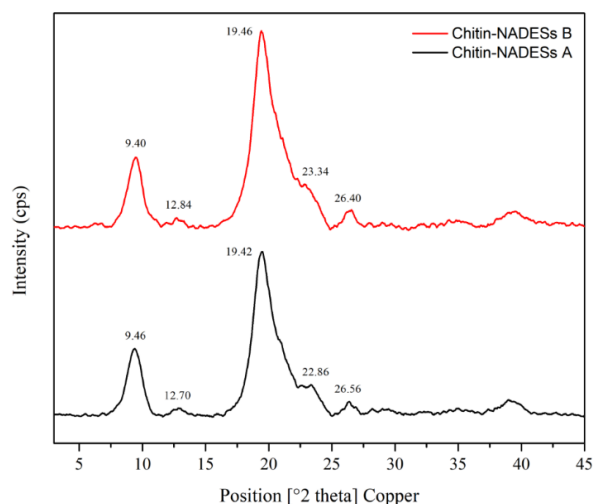


Figure 5. The diffractogram of chitin-NADES A and chitin-NADES B



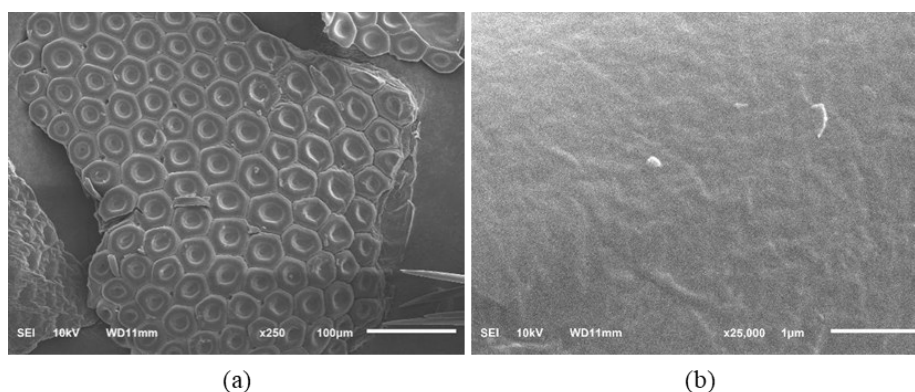


Figure 6. SEM images of chitin-NADES A and chitin-NADES B with (a) 250× magnification and (b) 25,000× magnification

### 3.5. Scanning Electron Microscope (SEM)

The surface morphology of chitin produced from *Hermetia illucens* was observed using SEM and shown in Figures 6a and 6b. First, chitin-NADES A and chitin-NADES B, at 250× magnification, showed the same structure as a honeycomb, based on the repetition of square, pentagonal, and hexagonal units (Figure 6a). Looking closer (25,000× magnification), the chitin-NADES A and chitin-NADES B show significant surface differences (Figure 6b). Various studies report that the surface morphology of chitin is divided into four types, namely (1) rough and solid surfaces without nano/microfiber and pores, (2) surfaces with a combination of nano/microfiber and pores (the most common morphology), (3) only fibrils, and porous surface (4) [44, 45]. Based on these four types, the chitin-NADES A and chitin-NADES B at 250× magnification show morphology (2), a surface combining nano/microfiber and pores. Meanwhile, the morphology at 25,000× magnification shows morphology (3), which is only fibrils.

### 4. Conclusion

The conclusion of this research is we have succeeded in synthesizing a choline chloride-based NADES with a density value of 0.99–1.09 g/cm<sup>3</sup>, viscosity of 3.39 mPa.s and 2.43 mPa.s. FTIR characterization from NADES shows that hydrogen bonds are formed between HBA and HBD at wave number values of 3307 cm<sup>-1</sup> and 3339 cm<sup>-1</sup>. TGA analysis the chitin-NADES A (350°C for decomposition with 10% residue left) has the best thermal stability compared to the chitin-NADES B (333°C for decomposition with 25% residue left).  $\alpha$ -chitin is characterized from BSF by XRD analysis at 9.46° and 19.42°. Based on morphology analysis in SEM showed that the chitin-NADES A and chitin-NADES B at 250× magnification show, a surface combining nano/microfiber and pores. Meanwhile, the morphology at 25,000× magnification shows morphology (3) which is only fibrils.

### Acknowledgment

We thank Universiti Teknologi PETRONAS for providing the grant so that the research can be carried out.

### References

- [1] Marguerite Rinaudo, Chitin and chitosan: Properties and applications, *Progress in Polymer Science*, 31, 7, (2006), 603–632  
<https://doi.org/10.1016/j.progpolymsci.2006.06.001>
- [2] Michael Kozma, Bishnu Acharya, Rabin Bissessur, Chitin, Chitosan, and Nanochitin: Extraction, Synthesis, and Applications, *Polymers*, 14, 19, (2022), 3989  
<https://doi.org/10.3390/polym14193989>
- [3] Julia L. Shamshina, Paula Berton, Robin D. Rogers, Advances in Functional Chitin Materials: A Review, *ACS Sustainable Chemistry & Engineering*, 7, 7, (2019), 6444–6457  
<https://doi.org/10.1021/acssuschemeng.8b06372>
- [4] Thomas Hahn, Aileen Roth, Ruomin Ji, Eric Schmitt, Susanne Zibek, Chitosan production with larval exoskeletons derived from the insect protein production, *Journal of Biotechnology*, 310, (2020), 62–67 <https://doi.org/10.1016/j.jbiotec.2019.12.015>
- [5] Imen Hamed, Fatih Özogul, Joe M. Regenstein, Industrial applications of crustacean by-products (chitin, chitosan, and chitoooligosaccharides): A review, *Trends in Food Science & Technology*, 48, (2016), 40–50  
<https://doi.org/10.1016/j.tifs.2015.11.007>
- [6] Thomas Hahn, Elena Tafi, Aman Paul, Rosanna Salvia, Patrizia Falabella, Susanne Zibek, Current state of chitin purification and chitosan production from insects, *Journal of Chemical Technology & Biotechnology*, 95, 11, (2020), 2775–2795  
<https://doi.org/10.1002/jctb.6533>
- [7] M. Barrett, S. Y. Chia, B. Fischer, J. K. Tomberlin, Welfare considerations for farming black soldier flies, *Hermetia illucens* (Diptera: Stratiomyidae): a model for the insects as food and feed industry, *Journal of Insects as Food and Feed*, 9, 2, (2023), 119–148 <https://doi.org/10.3920/JIFF2022.0041>
- [8] Andrea Scala, Jonathan A. Cammack, Rosanna Salvia, Carmen Scieuzo, Antonio Franco, Sabino A. Bufo, Jeffery K. Tomberlin, Patrizia Falabella, Rearing substrate impacts growth and macronutrient composition of *Hermetia illucens* (L.) (Diptera: Stratiomyidae) larvae produced at an industrial scale, *Scientific Reports*, 10, (2020), 19448  
<https://doi.org/10.1038/s41598-020-76571-8>
- [9] Law Yingyu, Wein Leo, Reversing the nutrient drain through urban insect farming—opportunities and

- challenges, *AIMS Bioengineering*, 5, 4, (2018), 226–237 <https://doi.org/10.3934/bioeng.2018.4.226>
- [10] Helena Čičková, G. Larry Newton, R. Curt Lacy, Milan Kozánek, The use of fly larvae for organic waste treatment, *Waste Management*, 35, (2015), 68–80 <https://doi.org/10.1016/j.wasman.2014.09.026>
- [11] L. A. Holmes, S. L. Vanlaerhoven, J. K. Tomberlin, Substrate Effects on Pupation and Adult Emergence of *Hermetia illucens* (Diptera: Stratiomyidae), *Environmental Entomology*, 42, 2, (2013), 370–374 <https://doi.org/10.1603/EN12255>
- [12] Lise Soetemans, Maarten Uyttbroek, Leen Bastiaens, Characteristics of chitin extracted from black soldier fly in different life stages, *International Journal of Biological Macromolecules*, 165, (2020), 3206–3214 <https://doi.org/10.1016/j.ijbiomac.2020.11.041>
- [13] Bojana Bradić, Uroš Novak, Blaž Likozar, Crustacean shell bio-refining to chitin by natural deep eutectic solvents, *Green Processing and Synthesis*, 9, 1, (2020), 13–25 <https://doi.org/10.1515/gps-2020-0002>
- [14] Wen-Can Huang, Dandan Zhao, Na Guo, Changhu Xue, Xiangzhao Mao, Green and Facile Production of Chitin from Crustacean Shells Using a Natural Deep Eutectic Solvent, *Journal of Agricultural and Food Chemistry*, 66, 45, (2018), 11897–11901 <https://doi.org/10.1021/acs.jafc.8b03847>
- [15] Huy Vu Duc Nguyen, Renko de Vries, Simeon D. Stoyanov, Chitin nanowhiskers with improved properties obtained using natural deep eutectic solvent and mild mechanical processing, *Green Chemistry*, 24, 9, (2022), 3834–3844 <https://doi.org/10.1039/D2GC00305H>
- [16] Mukesh Sharma, Chandrakant Mukesh, Dibyendu Mondal, Kamalesh Prasad, Dissolution of  $\alpha$ -chitin in deep eutectic solvents, *RSC Advances*, 3, 39, (2013), 18149–18155 <https://doi.org/10.1039/C3RA43404D>
- [17] Henni Vanda, Yuntao Dai, Erica G. Wilson, Robert Verpoorte, Young Hae Choi, Green solvents from ionic liquids and deep eutectic solvents to natural deep eutectic solvents, *Comptes Rendus Chimie*, 21, 6, (2018), 628–638 <https://doi.org/10.1016/j.crci.2018.04.002>
- [18] Wen-Can Huang, Dandan Zhao, Changhu Xue, Xiangzhao Mao, An efficient method for chitin production from crab shells by a natural deep eutectic solvent, *Marine Life Science & Technology*, 4, 3, (2022), 384–388 <https://doi.org/10.1007/s42995-022-00129-y>
- [19] Ruipu Xin, Suijian Qi, Chaoxi Zeng, Faez Iqbal Khan, Bo Yang, Yonghua Wang, A functional natural deep eutectic solvent based on trehalose: Structural and physicochemical properties, *Food Chemistry*, 217, (2017), 560–567 <https://doi.org/10.1016/j.foodchem.2016.09.012>
- [20] Liliana A. Rodrigues, Ivana Radojčić Redovniković, Ana Rita C. Duarte, Ana A. Matias, Alexandre Paiva, Low-Phytotoxic Deep Eutectic Systems as Alternative Extraction Media for the Recovery of Chitin from Brown Crab Shells, *ACS Omega*, 6, 43, (2021), 28729–28741 <https://doi.org/10.1021/acsomega.1c03402>
- [21] Dana I. M. Al-Risheq, M. S. Nasser, Hazim Qiblawey, Ibelwaleed A. Hussein, Abdelbaki Benamor, Choline chloride based natural deep eutectic solvent for destabilization and separation of stable colloidal dispersions, *Separation and Purification Technology*, 255, (2021), 117737 <https://doi.org/10.1016/j.seppur.2020.117737>
- [22] Yuli Piana Dewi, Ida Zahrina, Yelmida Yelmida, Karakteristik Nades (Natural Deep Eutectic Solvents), *Jurnal Online Mahasiswa (JOM) Bidang Teknik dan Sains*, 8, (2021), 1–5
- [23] Mohamad Shazeli Che Zain, Jen Xen Yeoh, Soo Yee Lee, Khozirah Shaari, Physicochemical Properties of Choline Chloride-Based Natural Deep Eutectic Solvents (NaDES) and Their Applicability for Extracting Oil Palm Flavonoids, *Sustainability*, 13, 23, (2021), 12981 <https://doi.org/10.3390/su132312981>
- [24] Orchidea Rachmaniah, Lailatul Jumiati Fazriyah, Nurul Hesti Seftiyani, M. Rachimoallah, Tailoring properties of acidic types of Natural Deep Eutectics Solvents (NADES): Enhanced solubility of curcuminoids from *Curcuma zedoria*, *MATEC Web of Conferences*, 2018 <https://doi.org/10.1051/mateconf/201815601011>
- [25] Agnese Cicci, Giorgia Sed, Marco Bravi, Potential of choline chloride-based natural deep eutectic solvents (NaDES) in the extraction of microalgal metabolites, *Chemical Engineering Transactions*, 57, (2017), 61–66 <https://doi.org/10.3303/CET1757011>
- [26] Ana P. R. Santana, Jorge A. Mora-Vargas, Taciana G. S. Guimarães, Clarice D. B. Amaral, Andrea Oliveira, Mario H. Gonzalez, Sustainable synthesis of natural deep eutectic solvents (NADES) by different methods, *Journal of Molecular Liquids*, 293, (2019), 111452 <https://doi.org/10.1016/j.molliq.2019.111452>
- [27] Yuntao Dai, Geert-Jan Witkamp, Robert Verpoorte, Young Hae Choi, Tailoring properties of natural deep eutectic solvents with water to facilitate their applications, *Food Chemistry*, 187, (2015), 14–19 <https://doi.org/10.1016/j.foodchem.2015.03.123>
- [28] Rekha Rose Koshy, Arunima Reghunadhan, Siji K. Mary, Prasanth S. Pillai, Seno Joseph, Laly A. Pothan, pH indicator films fabricated from soy protein isolate modified with chitin nanowhisiker and *Clitoria ternatea* flower extract, *Current Research in Food Science*, 5, (2022), 743–751 <https://doi.org/10.1016/j.crfcs.2022.03.015>
- [29] Parag S. Bhavsar, Giulia Dalla Fontana, Marina Zoccola, Sustainable Superheated Water Hydrolysis of Black Soldier Fly Exuviae for Chitin Extraction and Use of the Obtained Chitosan in the Textile Field, *ACS Omega*, 6, 13, (2021), 8884–8893 <https://doi.org/10.1021/acsomega.0c06040>
- [30] Kiki Adi Kurnia, Ardiani Putri Rahayu, Afifah Faradilla Islami, Yuly Kusumawati, I Gede Wenten, Anisa Ur Rahmah, Diana Vanda Wellia, Asep Saefumillah, Insight into the adsorption of dyes onto chitin in aqueous solution: An experimental and computational study, *Arabian Journal of Chemistry*, 15, 11, (2022), 104293 <https://doi.org/10.1016/j.arabjc.2022.104293>
- [31] Lokesh Sampath, Soibam Ngasotter, Layana Porayil, Amjad Khansaheb Balange, Binaya Bhusan Nayak, Shibu Eappen, K. A. Martin Xavier, Impact of extended acid hydrolysis on polymeric, structural and thermal properties of microcrystalline chitin, *Carbohydrate Polymer Technologies and Applications*,

- 4, (2022), 100252  
<https://doi.org/10.1016/j.carpta.2022.100252>
- [32] M. K. Rasweefali, S. Sabu, K. S. Muhammed Azad, M. K. Raseel Rahman, K. V. Sunooj, A. Sasidharan, K. K. Anoop, Influence of deproteinization and demineralization process sequences on the physicochemical and structural characteristics of chitin isolated from Deep-sea mud shrimp (*Solenocera hextii*), *Advances in Biomarker Sciences and Technology*, 4, (2022), 12–27  
<https://doi.org/10.1016/j.abst.2022.03.001>
- [33] A. Jayanegara, R. P. Haryati, A. Nafisah, P. Suptijah, M. Ridla, E. B. Laconi, Derivatization of chitin and chitosan from black soldier fly (*Hermetia illucens*) and their use as feed additives: An in vitro study, *Advances in Animal and Veterinary Sciences*, 8, 5, (2020), 472–477  
<http://dx.doi.org/10.17582/journal.aavs/2020/8.5.472.477>
- [34] Yin-Shen Lin, Shih-Hsiang Liang, Wen-Lin Lai, Ja-Xin Lee, Ya-Peng Wang, Yi-Tsz Liu, Szu-Han Wang, Meng-Hwan Lee, Sustainable Extraction of Chitin from Spent Pupal Shell of Black Soldier Fly, *Processes*, 9, 6, (2021), 976  
<https://doi.org/10.3390/pr9060976>
- [35] Hamou Moussout, Hammou Ahlafi, Mustapha Aazza, Mohamed Bourakhouadar, Kinetics and mechanism of the thermal degradation of biopolymers chitin and chitosan using thermogravimetric analysis, *Polymer Degradation and Stability*, 130, (2016), 1–9  
<https://doi.org/10.1016/j.polymdegradstab.2016.05.016>
- [36] K. Thongdonson, A. Boonmahitthisud, S. Tanpichai, Effect of sodium hydroxide on properties of shrimp-shells-extracted chitin nanofibers, *Journal of Physics: Conference Series*, 2175, (2022), 012019  
<https://doi.org/10.1088/1742-6596/2175/1/012019>
- [37] F. N. Jumaah, N. N. Mobarak, A. Ahmad, M. A. Ghani, M. Y. A. Rahman, Derivative of iota-carrageenan as solid polymer electrolyte, *Ionics*, 21, (2015), 1311–1320  
<https://doi.org/10.1007/s11581-014-1306-x>
- [38] Anuradha Saini, Anil Kumar, Parmjit Singh Panesar, Avinash Thakur, Potential of deep eutectic solvents in the extraction of value-added compounds from agro-industrial by-products, *Applied Food Research*, 2, 2, (2022), 100211  
<https://doi.org/10.1016/j.afres.2022.100211>
- [39] Jacob D. Goodrich, William T. Winter,  $\alpha$ -Chitin Nanocrystals Prepared from Shrimp Shells and Their Specific Surface Area Measurement, *Biomacromolecules*, 8, 1, (2007), 252–257  
<https://doi.org/10.1021/bm0603589>
- [40] G. Patrick Stahly, *Advantages of a Cu vs. Co X-ray Diffraction Source*, Triclinic Labs, 2012
- [41] Adam Waško, Piotr Bulak, Magdalena Polak-Berecka, Katarzyna Nowak, Cezary Polakowski, Andrzej Bieganski, The first report of the physicochemical structure of chitin isolated from *Hermetia illucens*, *International Journal of Biological Macromolecules*, 92, (2016), 316–320  
<https://doi.org/10.1016/j.ijbiomac.2016.07.038>
- [42] Huarui Wang, Kashif ur Rehman, Weijian Feng, Dan Yang, Rashid ur Rehman, Minmin Cai, Jibin Zhang, Ziniu Yu, Longyu Zheng, Physicochemical structure of chitin in the developing stages of black soldier fly, *International Journal of Biological Macromolecules*, 149, (2020), 901–907  
<https://doi.org/10.1016/j.ijbiomac.2020.01.293>
- [43] Cecile Brigode, Parinaz Hobbi, Hafez Jafari, Frederic Verwilghen, Emmanuel Baeten, Amin Shavandi, Isolation and physicochemical properties of chitin polymer from insect farm side stream as a new source of renewable biopolymer, *Journal of Cleaner Production*, 275, (2020), 122924  
<https://doi.org/10.1016/j.jclepro.2020.122924>
- [44] Micaela Triunfo, Elena Tafi, Anna Guarnieri, Rosanna Salvia, Carmen Scieuzo, Thomas Hahn, Susanne Zibek, Alessandro Gagliardini, Luca Panariello, Maria Beatrice Coltelli, Angela De Bonis, Patrizia Falabella, Characterization of chitin and chitosan derived from *Hermetia illucens*, a further step in a circular economy process, *Scientific Reports*, 12, (2022), 6613  
<https://doi.org/10.1038/s41598-022-10423-5>
- [45] Mi-Kyeong Jang, Byeong-Gi Kong, Young-Il Jeong, Chang Hyung Lee, Jae-Woon Nah, Physicochemical characterization of  $\alpha$ -chitin,  $\beta$ -chitin, and  $\gamma$ -chitin separated from natural resources, *Journal of Polymer Science Part A: Polymer Chemistry*, 42, 14, (2004), 3423–3432  
<https://doi.org/10.1002/pola.20176>
- [46] Murat Kaya, Muhammad Mujtaba, Hermann Ehrlich, Asier M. Salaberria, Talat Baran, Chris T. Amemiya, Roberta Galli, Lalehan Akyuz, Idris Sargin, Jalel Labidi, On chemistry of  $\gamma$ -chitin, *Carbohydrate Polymers*, 176, (2017), 177–186  
<https://doi.org/10.1016/j.carbpol.2017.08.076>
- [47] Chu Yong Soon, Yee Bond Tee, Choon Hui Tan, Abdul Talib Rosnita, Abdan Khalina, Extraction and physicochemical characterization of chitin and chitosan from *Zophobas morio* larvae in varying sodium hydroxide concentration, *International Journal of Biological Macromolecules*, 108, (2018), 135–142  
<https://doi.org/10.1016/j.ijbiomac.2017.11.138>
- [48] Warayuth Sajomsang, Pattarapond Gonil, Preparation and characterization of  $\alpha$ -chitin from cicada sloughs, *Materials Science and Engineering: C*, 30, 3, (2010), 357–363  
<https://doi.org/10.1016/j.msec.2009.11.014>
- [49] Sevil Erdogan, Murat Kaya, High similarity in physicochemical properties of chitin and chitosan from nymphs and adults of a grasshopper, *International Journal of Biological Macromolecules*, 89, (2016), 118–126  
<https://doi.org/10.1016/j.ijbiomac.2016.04.059>